Contents

Acknowledgements

After about 20 years this is my rst time back into mathematics and its been very interesting and challenging! My classmates and various lecturers over the last two years have been very friendly and supportive so thanks go to them. Thanks goes to my workmates who have been most accommodating with time o work and working strange hours at times. Thanks also goes to the University of Reading for part-funding the masters. A special thanks to Louise for being very supportive of the two years while also having her own study to contend with. Most of all, thanks goes to my supervisor Mike Baines for all the positive meetings and help given. Many a time I have left his room with a considerably more positive frame of mind than when I entered, and plenty of notes.

Declaration

I con rm that this is my own work and the use of all materials from other sources have been properly and fully acknowledged.

Signed................................. Date............................

1 Abstract

Richards' equation describing soil water ow is a highly nonlinear PDE and as such can only be solved numerically except for a small number of special conditions. Two schemes were considered here; the Crank Nicolson scheme with a nonlinear solver and a conservation-based moving mesh scheme. Four realistic scenarios were chosen to test the the schemes; i) a shallow moving water table, (ii) unsaturated in ltration on dry soil, (iii) ponded in ltration on dry soil, and (iv) in ltration into layered soil. The schemes were found to work well, with the ponded in ltration being the most challenging in terms of size of timestep required. Unstable ows were brie y considered where in ltrating water is held up momentarily. A mechanism for explaining this waiting time is described.

2 Introduction

The aim of this project was to implement a robust xed mesh scheme and a conservative-based moving mesh (MM) scheme for solving Richards'equation (RE) for four realistic and challenging boundary conditions: (i) a shallow, moving water table, (ii) unsaturated in ltration, (iii) ponded in ltration, and (iv) in ltration into layered soil. Two soils were simulated which were chosen to be near the two ends of the textural spectrum; sandy and clayey soils. The xed mesh scheme is the nonlinear Crank Nicolson (CNi) scheme which is a semi-implicit method requiring an iterative preocedure. Fixed mesh implicit schemes have been used extensively in the literature [4] for solving RE and more recently have incorporated time adaption schemes [5]. The performance of the CNi scheme and the requirement of adaptive timestepping is investigated here. The MM scheme investigated here is not a common form of the adaptive mesh schemes used for solving RE. Most adaptive mesh schemes are concerned with reducing truncation errors and increasing model e ciency [6]. The advantage of the MM scheme is the in-

-based, and mixed, are given.

In Chapter 3, the schemes are described. The derivation of the CNi scheme starts with the explicit scheme and progresses to the linear Crank-Nicolson scheme (with K

3 Background theory - soil physics

3.1 Soil Structure

Soil is a solid lattice made up of mineral and organic fractions. The mineral fraction generally makes up the majority by volume and consists of particles of diameters varying from clay (> 2 m) to coarse sand (up to 2 mm). The relative proportion of these particle sizes and organic matter (which acts as a glue to bond particles togther to form aggregates) largely determines the range of pore sizes present in the soil. It is this distribution of pore sizes that greatly influences water storage and movement.

Water can be present in soils in its three phases, but most often in the liquid and gaseous phases only. Water movement in soil is mainly due to

3.2 Soil water - de nitions

There are two main concepts related to describing the amount or state of water in soils; (i) volumetric water content, $(m^3 m^{\ 3}$

3.5 Water flow in soils - Darcy's Law

The movement of water occurs in soil when gradients of ψ develop from inputs/removal of water from precipitation/evaporation at the soil surface or root uptake in the soil profile. Water flows from regions of high to low values of ψ and is described by Darcy's Law:

$$q = -K\left(\frac{\partial \psi}{\partial z} + 1\right) \tag{3.4}$$

where q is the flow rate (ms^{-1}), K is the hydraulic conductivity (ms^{-1}), and z is usually the depth below the soil surface (m). The hydraulic conductivity is a highly non-linear function of ψ (or θ) and is difficult to measure particularly at lower θ. However, K is found to be strongly connected to the SMC. Because of this, the expression for K is derived directly from expressions for the SMC, e.g. from equation (3.2):

$$K = K_s\left(\frac{\theta}{\theta_s}\right)^{n1} \quad or \quad K = K_s\left(\frac{\psi_e}{\psi}\right)^{n2} \tag{3.5}$$

where $n1 = 2b + 3$ and $n2 = 2 + 3/b$, and b is from equation (3.2).

3.6 Derivation of Richards' equation

The mass continuity equation

$$\frac{\partial q}{\partial z} = \frac{\partial \theta}{\partial t} \tag{3.6}$$

is combined with Darcy's Law (equation 3.4) to obtain Richards' equation (RE)

$$\frac{\partial \theta}{\partial t} = \frac{\partial}{\partial z}\left[K\left(\frac{\partial \psi}{\partial z} - 1\right)\right]. \tag{3.7}$$

conserved is the physical quantity , the gradient being expressed in terms of , and K is a function of . Other forms of RE are the -based and -based versions shown below:

$$
\begin{aligned}
\frac{@}{@t} &= \frac{@}{@z} \; K \quad D\frac{@}{@z} \quad 1 \\
C\frac{@}{@t} &= \frac{@}{@z} \; K \quad \frac{@}{@z} \quad 1
\end{aligned}
\qquad (3.8)
$$

where $D = @ \; =@$ and $C = @ \; =@$ from applying the product rule. The above forms of RE have been used extensively in the literature. The mixed and -based forms are best for conservation of mass, parrticularly when sharp moisture gradients are present, and the mixed and -based forms are necessary for saturated conditions and layered soil [4]. During saturated conditions when water is ponding on the soil surface, the value of at the surface equals the depth of free water on the surface. This positive potential cannot be portrayed using as the driving variable (equation 3.8a). For layered soil, and not is the continuous variable down the soil pro le.

3.7 Boundary conditions

For one dimensional vertical ow, only top and bottom boundary conditions exist as depicted in the schematic below (Figure 3.3). The top boundary or soil surface is exposed to the highly variable atmospheric conditions so can change rapidly. For the most part, the top boundary has a ux of water passing through it either downward from in ltration as liquid water or upward from evaporation in the vapour phase. If ponding does occur, when the precipitation rate is greater than the maximum in ltration rate (see later in next chapter), $= h$ where h is the depth of water on the soil surface. When considering solving RE, the top boundary is predominantly a Neumann or ux bounday condition, but for some soil types and environmental conditions, a Dirichlet boundary condition can occur. The bottom boundary is often deep enough such that the gradient is considered to be zero, or for a shallow water table, the value of or being equal to that at saturation.

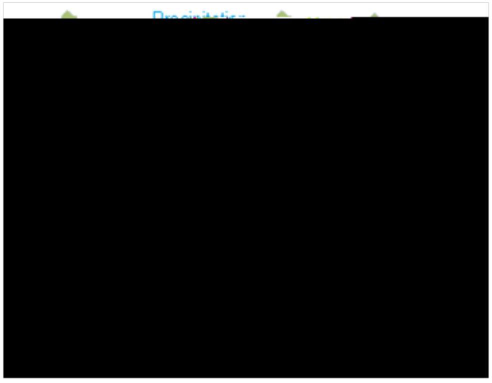

Figure 3.3: Schematic showing the vertical nature of water ows [1]

4 Numerical schemes for solving Richards' equation

Since the 1970's, inceasingly complex numerical schemes have been developed to solve RE. The highly non-linear nature of RE requires that numerical rather than exact solutions be sought. Due to the complex nature of real soils and environmental conditons, improvements to numerical schemes to increase the e ciency, stability and accuracy is ongoing. The schemes can be broadly grouped into schemes with xed meshes (FM) and those with adaptive meshes (AM). The former are generally simpler to design and implement with the latter a relatively new concept. Only nite difference methods are investigated here since only one dimensional ows are considered. Techniques such as nite elements do not have appreciable advantages over nite di erences in one dimension. This brief review on numerical schemes follows that of [5] who produced quite an extensive review on numerical solutions to RE. The xed mesh methods used are a Crank-Nicolson linear scheme and a fully implicit nonlinear scheme using iterative methods such as Picard or Newton-Raphson [4]. These two methods are explored in more detail in the next section. A later improvement to these schemes was to add in an adaptive time-step procedure. Two main methods exist for varying the time step, h [6]; (i) empirical - based on the number of iterations per time step, and (ii) error-based where estimates of the truncation error are obtained and the time step adjusted accordingly. In addition, the order of the time stepping scheme can be varied. The AM techniques can be grouped into three types; (i) moving mesh points, (ii) adding/subtracting mesh points, and (iii) increasing the order. Often a combination of the above techniques is used. As with the xed mesh methods, adaptive time stepping can be included, producing some complex but robust schemes [5]. The main advantage of AM over FM schemes is the combination of increased accuracy and stability as well as e ciency. The FM schemes can be made more accurate by decreasing the distance between mesh points (z) and the time step, but this decreases the e ciency. With AM, h (and z) can be decreased only when required, which can be for relatively small periods of time. Larger-405( )]TJ/F22 11M02.678 0 Td [(sE2e2(sc31.9552 T

4.1 Fixed mesh methods

Often at eld-scale or larger, variation in the variables and occurs mainly in the vertical dimension since horizontally the surface appears uniform. For larger scales, the region can be divided up into smaller areas of similar surface type, each with a one-dimensional ow scheme.

A mesh is rst inserted on the vertical soil pro le (z direction) usually with $z = 0$ at the soil surface (see gure 4.1 below). The spacings (z) often increase in the positive z direction with z 1 cm at $z = 0$ and z 1 m at the base of the pro le. These spacings re ect the relative temporal and spatial variation of and down the pro le. The -based RE (see previous chapter) is discretised in the following sections since it is used later in the Results chapter, but the analysis will be very similar for the other versions of RE. The rest of the chapter is devoted to the description of various simple numerical schemes for RE which can be represented here as $C\ _t = (K(\ _z\ \ 1))_z$. The rst and simplest is the explicit scheme where the rst derivative in time ($_t$) is approximated by the rst order forward di erence and the second order derivative in space approximated by a second order forward di erence. The subsequent schemes investigated; various forms of the Crank-Nicolson scheme and fully implicit schemes, are based on this explicit discetisation.

Explicit scheme

The basic explicit discretisation of the -based RE is

$$C_i^{n+1}$$

8.45--402312 Td [(i)]TJ/620 7.9701

Figure 4.1: Soil pro le divided into layers with and centred on the mesh points.

where i and n are the space and time indices respectively, $z_i = z_i \quad z_{i \; 1}$, and $\overline{z_i} = 1{=}2(\; z_i + \; z_{i \; 1})$ (see Figure f41). This scheme is rst order in time and second order in space and according to the stability criterion, the maximum timestep $t_{max} = 1{=}2 \; z^2{=}K_{max}$. Equation (4.1) can be easily rearranged to have all the known terms (at *nth* timestep) on the RHS and $^{n+1}$ on the LHS. Values for are obtained by advancing through time. Implementing this in code requires a space loop nested in a time loop.

The boundary conditions must be included. These are discussed below for the explicit method but equally apply to the subsequent schemes and can be readily implemented. Both the top and bottom boundaries for the

Figure 4.2: Schematic showing ponded in ltration into soil.

where = 1=2. This scheme is 2nd order in time and space. Note that for = 0, equation (4.5) reverts back to the explicit scheme of equation (4.1). The K terms are evaluated at timestep n so equation (4.5) is still a set of linear algebraic equations as with the explicit scheme above. However, the RHS contains $n+1$ terms so some rearranging of equation (4.5) is required to separate the n (on RHS) and the $n+1$ (on LHS) terms:

$$a_i^n \; {}^{n+1}_{i\;1} + b_i^n \; {}^{n+1}_{i} + c_i^n \; {}^{n+1}_{i+1} = r_i^n \qquad (4.6)$$

where

$$a_i^n = \frac{tK^n_{i\ \frac{1}{2}}}{C_i^n\ \ z_{i\ \ 1}\ \ \overline{z_i}}(1\qquad)$$

$$b_i^n = 1 + (1\qquad)\frac{tK^n_{i\ \frac{1}{2}}}{C_i^n\ \ z_{i\ \ 1}\ \ \overline{z_i}}\quad (1\qquad)\frac{tK^n_{i+\frac{1}{2}}}{C_i^n\ \ z_i\ \ \overline{z_i}}$$

$$c_i^n = \frac{tK^n_{i+\frac{1}{2}}}{C_i^n\ \ z_i\ \ \overline{z_i}}(1\qquad)$$

$$r_i^n = {}_i^n \frac{}{C_i^n\ \ \overline{z_i}}\quad K^n_{i+\frac{1}{2}}\ \frac{{}^n_{i+1}\qquad {}^n_i}{z_i}\quad 1\qquad K^n_{i\ \frac{1}{2}}\ \frac{{}^n_i\qquad {}^n_{i\ 1}}{z_i}\quad 1$$

$$\frac{tK^n_{i+\frac{1}{2}}}{C_i^n\ \ \overline{z_i}} + \frac{tK^n_{i\ \frac{1}{2}}}{C_i^n\ \ \overline{z_i}}$$

This can all be written in matrix form:

$$\mathsf{A}\_ = \underline{r}$$

where

$$\mathsf{A} = \begin{pmatrix} b_0 & c_0 & 0 & \cdots & & 0 \\ a_1 & b_1 & c_1 & & & \vdots \\ 0 & \ddots & \ddots & \ddots & & 0 \\ \vdots & & & a_{I\ 1} & b_{I\ 1} & c_{I\ 1} \\ 0 & \cdots & & 0 & a_I & b_I \end{pmatrix}$$

In (A) above, a_i,b_i, and c_i terms make up the lower, middle and upper diagonals of A respectively. The vector _ holds the ${}_i^{n+1}$ variables and $\underline{r}$ holds the known variables (at time level n) plus boundary conditions. Since A is tridiagonal (see above) and $|b_i| > |a_i|$

lated at the previous iteration step. As the iteration proceeds, $\underline{F} \to 0$ as $\underline{\psi}^{n+1;p+1} \to \underline{\psi}^{n+1;p}$. The elements of J are calculated at the p iteration level.

$$J = \begin{pmatrix} \frac{\partial F_0}{\partial \psi_0} & \frac{\partial F_0}{\partial \psi_1} & 0 & \cdots & & 0 \\ \frac{\partial F_1}{\partial \psi_0} & \frac{\partial F_1}{\partial \psi_1} & \frac{\partial F_1}{\partial \psi_2} & & & \vdots \\ 0 & \ddots & \ddots & \ddots & & 0 \\ \vdots & & & \frac{\partial F_{I-1}}{\partial \psi_{I-2}} & \frac{\partial F_{I-1}}{\partial \psi_{I-1}} & \frac{\partial F_{I-1}}{\partial \psi_I} \\ 0 & \cdots & & 0 & \frac{\partial F_I}{\partial \psi_{I-1}} & \frac{\partial F_I}{\partial \psi_I} \end{pmatrix}$$

The elements of $\underline{F}$ are calculated at the n and $n+1/2; p$ levels.

$$F_i = \psi_i^{n+1;p} - \psi_i^n + \frac{\theta \Delta t}{C_i^{n+\frac{1}{2};p}\,\overline{\Delta z_i}} \left(K_{i+\frac{1}{2}}^{n+\frac{1}{2};p} \left(\frac{\psi_{i+1}^n - \psi_i^n}{\Delta z_i} - 1 \right) - K_{i-\frac{1}{2}}^{n+\frac{1}{2};p} \left(\frac{\psi_i^n - \psi_{i-1}^n}{\Delta z_i} - 1 \right) \right)$$
$$+ \frac{(1-\theta)\Delta t}{C_i^{n+\frac{1}{2};p}\,\overline{\Delta z_i}} \left[K_{i+\frac{1}{2}}^{n+\frac{1}{2};p} \left(\frac{\psi_{i+1}^{n+1;p} - \psi_i^{n+1;p}}{\Delta z_i} - 1 \right) - K_{i-\frac{1}{2}}^{n+\frac{1}{2};p} \left(\frac{\psi_i^{n+1;p} - \psi_{i-1}^{n+1;p}}{\Delta z_i} - 1 \right) \right] \tag{4.10}$$

The matrix J is diagonally dominant and hence non-singular, so can be inverted to solve equation 4.9.

4.2 Moving mesh - velocity based

A moving mesh scheme using a velocity-based approach is also applied to the vertical soil profile. This type of scheme is particularly useful where there are moving boundaries in the physical system. For the soil environment, two such cases exist: (i) a moving water table at the bottom boundary, and (ii) ponded infiltration at the top boundary. The former can occur in areas such as flood plains or water meadows where the water table (depth below soil surface) is largely driven by the river levels nearby. The water table can therefore fluctuate relatively quickly. Ponded infiltration occurs when the rate of rainfall is greater than the maximum rate of infiltration for the

Figure 4.3: Moving mesh scheme illustrated for the three scenarios described in the text.

(4.17) becomes:

$$\frac{dz_i}{dt} = \frac{1}{\ } \left\{ \left(K\frac{\partial}{\partial z} \quad 1 \right)^{b} e \qquad K\frac{\partial}{\partial z} \quad 1 \quad ^{z_i} + e \right\} \tag{4.18}$$

where $da{=}dt = 0$ and $db{=}dt = 0$ since there is no imposed boundary velocities and e is the prescribed boundary condition at a which is set by the external atmospheric conditions. For scenario (ii), equation (4.17) becomes:

$$\frac{dz_i}{dt} = \frac{1}{\ } \left\{ {}_i \quad \left(K\frac{\partial}{\partial z} \quad 1 \quad ^{b} e + {}_b\frac{\partial b}{\partial t} \right) \qquad K\frac{\partial}{\partial z} \quad 1 \quad ^{z_i(t)} + e \right\} \tag{4.19}$$

where $\partial b{=}\partial t$ is the velocity of the top of the moving water table and ${}_b$ is the value of at b. Finally for scenario (iii),

$$\frac{dz_i}{dt} = \frac{1}{\ } \left\{ {}_i \quad \left(K\frac{\partial}{\partial z} \quad 1 \quad ^{b} e \qquad {}_a\frac{\partial a}{\partial t} \right) \qquad K\frac{\partial}{\partial z} \quad 1 \quad ^{z_i(t)} + e + {}_a\frac{\partial a}{\partial t} \right\} \tag{4.20}$$

The equations (4.18)-(4.20) show how the mesh points move under the scenarios (i)-(iii). Discretisation of equation (4.18) (equations (4.19) and (4.20) are similarly discretised but not shown here) is giv9F1585+

5 Solutions to Richards' equation

This chapter mainly focusses on the performances of the nonlinear iterative Crank Nicolson (CNi) and moving mesh (MM) schemes under various realistic situations:

(i) moving water table near the soil surface

(ii) infiltration into dry soil; unsaturated and ponded infiltration

(iii) infiltration into layered soil

The above cases represent some of the more challenging areas in soil water flow with respect to model stability and accuracy. The output from the other schemes described in the previous chapter give similar results to the CNi scheme provided suitable timesteps are applied. The Newton Raphson iteration method is mainly considered here with the Picard method giving virtually identical results but with more iterations required [10]. The sizes of timestep chosen here is a compromise between accurate solutions and efficient use of computer resource. An hourly timestep is chosen whenever possible as this gives good diurnal resolution and will generally give good results in most situations [11]. The size of the timestep used in the following analysis depends on the level of accuracy calculated.

50

Figure 5.2: Sinusoidally varying water table with the moving mesh scheme.

soil types; a sandy and clayey soil. Table 5.1 below shows values for typical soil hydraulic parameters. The timesteps chosen were 600s for the sandy

Table 5.1: Parameter values.

	Sandy soil	Clayey soil	units

[redacted]

Figure 5.3: Results from xed mesh schemes with varying water table for sandy soils.

Figure 5.4: Results from xed mesh schemes with varying water table for clayey soils.

Figure 5.5: Results from moving mesh scheme with varying water table for sandy soil.

Figure 5.6: Results from moving mesh scheme with varying water table for clayey soil.

Table 5.2: % error values in pro le water between the schemes.

time(hr)	z_w (m)	% error sand	% error clay
10	1:71	1:70	1:50
20	1:07	1:60	1:57
30	0:53	1:40	1:60
40	0:47	1:22	1:49
50	0:94	1:18	1:40
100	0:61	1:50	1:74

Figure 5.7: Results from moving mesh scheme showing mesh points moving with time.

was calculated for the xed mesh scheme using the following equation:

$$\text{water balance} = (\text{change in pro le water} + \frac{da}{dt}\ _l + q_0 + q_l)\ \ t = 0 \quad (5.2)$$

where q_l and q_0 are the uxes at the boundaries, and $da{=}dt$ is the velocity of the water table. It was found that the LHS of equation (5.2) was of the same magnitude as the individual terms on the RHS. The xed scheme in this case did not seem to conserve whereas this is inherent in the derivation of the moving mesh scheme. For the xed mesh schemes, the treatment of the lower boundary could be improved. Currently the last mesh point (I) moves with the water table depth a, so that the spacing between mesh points I and $I + 1$ can have values between 0 and z where z is the original mesh spacing (and equal to the spacings between the other mesh points).

5.2 In ltration into dry soil

Rain falling onto dry soil will produce large gradients of water below the soil surface. Depending on the intensity of the rain and the type of soil, either unsaturated or saturated (ponded) ow into the soil will result. A ne-textured soil (clays) will have more chance of ponded in ltration since this soil typically has a much lower saturated hydraulic conductivity than coarser sandy soils. If the rainfall rate is greater than the maximum in l-tration rate for a particular soil, then saturated or ponded in ltration will occur. From a modelling perspective, the top boundary condition will be a ux or Neumann condition for unsaturated in ltration and a Dirichlet condition for ponded ow.

Unsaturated in ltration

The top boundary condition simulated a constant rain event at

Figure 5.8: Fixed mesh solutions for in ltration onto sandy soil.

Figure 5.9: Fixed mesh solutions for in ltration onto clayey soil.

respectively with t given as 3600*s* for each. Figures 5.8 and 5.9 agree well, with the moving mesh producing slightly faster rate of water in ltration. The number of iterations per timestep as well as the mass balance error is shown in Figures 5.10 and 5.11. In both gures, the initial values for these is high coinciding with initially high moisture gradients. The initially high values quickly decay to low levels as time progresses so an hourly timestep could be suitable here, especially for the ner textured soils. Higher rainfall rates could pose more of a problem which is shown in the next section for ponded in ltration. The results for the MM scheme is given in Figures

Figure 5.10: Iterations per timestep and % error for the xed mesh scheme (CNi) for sandy soil.

5.12 and 5.13. These show good similarity with the CNi scheme 1(igh)]TJ 0 -l]TJ 09(of)h

Figure 5.12: Moving mesh solutions for infiltration onto sandy soil.

Figure 5.13: Moving mesh solutions for infiltration onto clayey soil.

Table 5.3: % error values in pro le water between schemes.

time(hr)

Figure 5.15: Fixed mesh solutions for ponded in ltration onto sandy soil.

Figure 5.16: Fixed mesh solutions for ponded in ltration onto clayey soil.

Figure 5.17: Iterations per timestep for the CNi scheme for the sandy soil

Figure 5.18: Iterations per timestep for the CNi scheme for the clayey soil

Figure 5.19: Moving mesh solution for ponded in ltration onto sandy soil.

Figure 5.20: Moving mesh solution for ponded in ltration onto clayey soil.

Figure 5.21: Moving mesh solution for sandy soil showing position of mesh points with time.

generally have large discontinuities in value down a layered pro le. Here a soil with two contrasting soil layers; clay over sand, initially dry, is subjected to continuous in ltration at 20 $mm\ hr^{1}$. The clay over sand soil pro le was chosen as this situation can cause the wetting front (under moderate in ltration rates) to be held up [14]. This causes the moisture gradient at the clay/sand boundary to become steeper. Unstable ows can result which culminate in ' ngered ows' through the sand. This greatly enhances the rate of ow of water further down the pro le which has implications for leaching of contaminants into the groundwater [15].

The MM scheme for the whole pro le would not be useful with a stationary boundary in the middle of the pro le. So two types of methods were investigated here, (i) a xed mesh is inserted on the whole soil pro le, and (ii) a moving mesh was placed on the top soil and a xed mesh on the bottom soil layer. Figure 5.22 shows the results from the xed mesh method.

The mass balance error is calculated by comparing the input of water to the simulated change in pro le water content (Table 5.4) which shows after an initial value of 8:9% decreases quickly. This value remained under 1% for the remainder of the simulation even when the wetting front passed through the soil pro le discontinuity. Figure 5.23 shows results from the second

Table 5.4: % Mass balance error for CNi scheme.

time(hr)	% error
1	8:9
2	3:0
3	1:1
4	1:1
5	0:9

Figure 5.22: Fixed mesh solution for in ltration into layered soil; clayey over sandy soil. Time in hours listed on right

method which is similar to the CNi only method. A considerably smaller timestep was required for the second method (30 *s* compared to 3600 *s*)

Figure 5.23: Moving mesh solutions for in ltration into layered soil; clayey over sandy soil. Time in hours listed on right

since the MM scheme is explicit. The potential for the MM scheme to be used at the boundary to improve the treatment of the gradients is investigated further in the next chapter. As water builds up at the boundary and the moisute gradient increases, the spacing between the mesh points

6 Investigation into waiting times

Vertical flow only is considered in the following analysis. It has been found in practice that water infiltrating into soil at a 'medium' rate (a rate sufficiently below the maximum rate so gravity forces are not dominating, and high enough so matric forces are not dominating) can cause unstable flows at the wetting front. This is common in layered soils where a fine-textured soil overlies a coarse-textured one. In this case, the advance of water is held up at the boundary of these two soil types and after some time breaks through the boundary in 'fingers' of flow. This has also been observed within coarse-textured soils which are initially dry and then subjected to water infiltration. In both cases there is a period of time where the wetting front is stationary followed by water flow through this point, resulting in 'fingered' flow. Water flow in soil is governed by Darcy's Law:

$$q = -K\left(\frac{\partial\psi}{\partial z} + 1\right) \tag{6.1}$$

where the hydraulic conductivity (K) is given here as:

$$K = K_s\left(\frac{\theta}{\theta_s}\right)^{n} \tag{6.2}$$

The relationship between water potential (ψ) and water content (θ) is given here as:

$$\frac{\psi}{\psi_e} = \left(\frac{\theta}{\theta_s}\right)^{-b} \tag{6.3}$$

where $_e$, $_s$, b, and n are constants and $n = 2 + 3b$. If we now consider equation (6.1) with only as the independant variable, using the chain rule and di erentiating equation (6.3) with respect to , equation (6.1) becomes:

$$q = (A \; ^{n \; b \; 1} \; _z + B \; ^n) \qquad (6.4)$$

where $A = bK_s \; _e \; ^b_s \; ^n$ and $B = K_s \; ^n$. Hence the Darcy velocity (v) is given by:

$$v = (A(\; ^{n \; b \; 1})_z + B \; ^{n \; 1}) \qquad (6.5)$$

For the purposes of investigating this 'waiting' behaviour of the wetting front discussed above, the constants in equation (6.5) are set to unity with $b = 2$ giving:

$$v = (\; ^5)_z \quad ^7 \qquad (6.6)$$

and the initial conditions are given by

$$= \begin{matrix} (1 \quad z) & \text{if } z \quad 1; \\ 0 & \text{if } z > 1 \end{matrix}$$

with = 1, consistent with the boundary condition. The Darcy velocity $v > 0$ for $z < 1$ and $v = 0$ at $z = 1$. From equation (6.6) ,for v to become greater than zero at $z = 1$, $_z$ must become in nite at that point. Figure 6.1 shows the initial conditions with the equivalent of normalised and then at some time T where the gradient has increased by decreasing . The behaviour of the v when $_z \; ! \; 1$ is now investigated further by substituting the initial conditions into equation (6.6) giving:

$$v = 5 \; (1 \quad z)^{5 \quad 1} \quad (1 \quad z)^7 : \qquad (6.7)$$

As time advances, the value of will decrease and at $z = 1$, there are three possible outcomes for v depending on the value of :

1. for 5 < 1, $\quad v \; ! \; 1$

Figure 6.1: Gradient at the point $x = 1$ at t=0 and increasing at time t=T in response to decreasing from 1 to 0.3.

2. for 5 > 1, $v \to 0$

3. for 5 $= 1$, v is nite

Hence, when the shape of the wetting front changes, decreases until case (3) above is reached when v at $z = 1$ becomes nite and moves in the direction of increasing z.

When solving the problem above numerically using a velocity-based moving mesh technique, the mesh points are required to move according to the discrete form of equation (6.8):

$$\left.\frac{\partial z}{\partial t}\right|_i \quad \frac{z_i^{n+1} \quad z_i^n}{t} = \frac{5_{i+\frac{1}{2}} \quad 5_{i-\frac{1}{2}}}{z_{i+\frac{1}{2}} \quad z_{i-\frac{1}{2}}} \, 7_i \qquad (6.8)$$

The value of at mesh point $z = 1$ ($i = I$(to)-32(the)erm-414(6w)27(e)(6w)residuale6w6w6we6w

I increases and this is shown in Figure 6.2. The mesh points near point I decrease with time as shown in Figure 6.3 and this is useful in simulating the large (in nite in theory) gradient necessary at point I for velocity to increase appreciably above zero. The numerical solution does therefore appear to mimic the analytical analysis above.

Figure 6.2: Moving mesh scheme mimicing the waiting time as predicted from theory.

Figure 6.3: Mesh points position with time. The spacings decrease dramatically near point I as the velocity at I noticeably increases.

7 Conclusions and Future work

7.1 Conclusions

resource available will determine the answer. Except for the ponding in I-by either an empirical approach based on the number of iterations per timestep or using a mechanistic approach which is based on an estimate of the truncation error at each timestep [17]. This adaptive scheme could be simply added with little internal change to CNi scheme.

(ii) An existing study on the Oxfordshire floodplains (joint project by the University of Reading and CEH Wallingford) has as one of its objectives to develop a combined soil water and heat flow model which is to interface with an existing above-ground water and energy balance model. The work done here to implement a robust implicit finite difference scheme for solving Richards' equation could be further ad-

Bibliography

[1] Dr. Anne Verhoef, School of Human and Environmental Sciences, University of Reading

[2] Brookes R.H. and Corey A.T. Hydraulic properties of porous media: Hydrology Papers, Colorado State University, 24 pages,1964

[3] van Genutchen M.Th. A closed-form equation for predicting the hydraulic conductivity of unsaturated soils. *Soil Sci. Am. J.* 44:892-898, 1980

[4] T.P. Clement, W.R. Wise, F.J. Molz. A physically-based, two dimension nite di erence algorithm for modelling variably saturated ow. *J. of Hydrol* 161, 71-90, 1994

[17] Kavetski D., P. Binning. and S. W. Sloan. Adaptive backward Euler time stepping with truncation error control for numerical modelling of unsaturated uid ow. *Int. J. Numer. Meth. Engng* 2002; 53:13011322